JOURNAL OF APPLIED ELECTROCHEMISTRY 9 (1979) 603–613

Zinc deposit structures obtained from synthetic zinc chloride electrolyte

D. J. MACKINNON, J. M. BRANNEN

Metallurgical Chemistry Section, Physical Sciences Laboratory, CANMET, Department of Energy, Mines and Resources, Ottawa, Canada

V. I. LAKSHMANAN

Research and Development Division, Eldorado Nuclear Ltd, Ottawa, Canada

Received 22 September 1978

Zinc deposits electrowon from synthetic zinc chloride electrolyte were characterized by a morphology which featured clusters of large platelets with rounded edges and by a preferred crystallographic orientation, namely (0 0 2) (1 0 3) (1 0 5). These deposit characteristics persisted over a wide range of experimental conditions which included variations in the current density and changes in anode material, cell design, and the zinc and hydrochloric acid concentrations. Although the addition of HCl to the electrolyte improved the physical characteristics of the deposit, it did not alter the deposit morphology or orientation. The addition of animal glue or tetrabutylammonium chloride resulted in smooth, compact deposits having a (1 1 0) orientation at 0·24 M H^+. Jaguar C-13 additions gave a (1 1 2) orientation, while gum arabic and tetraethylammonium chloride only affected the grain size. The various deposit morphologies and orientations obtained showed only some correspondence to changes occurring in the zinc deposition polarization voltages. The presence of metallic impurities, Cu, Co, Fe, and Sb, caused the morphology and orientation of the deposits to become more basal and the current efficiency to decrease. The presence of Cd resulted in a (1 1 2) (1 1 4) orientation and Pb gave a (1 0 1) orientation.

1. Introduction

Chemical and electrochemical leaching processes using chloride solutions ($FeCl_3$, HCl, $CuCl_2$) and dry chlorination with Cl_2 gas followed by leaching of the resultant chlorides are some of the methods which are under active investigation for treating fine-grained Zn–Pb–Cu–Fe sulphide ores and concentrates [1]. These processes eventually result in an impure zinc chloride liquor which, after purification using either solvent extraction or conventional zinc dust cementation, could yield a chloride electrolyte suitable for zinc electrolysis. Although solvent extraction technology also offers the possibility of converting the zinc chloride electrolyte to the sulphate system from which zinc could be recovered by conventional electrowinning [2–4], direct electrolysis of zinc chloride has the potential advantage that the chlorine gas generated at the anodes could be recycled to the dry chlorination step or used to regenerate the aqueous leaching medium.

Zinc was formerly produced on an industrial scale by the electrolysis of zinc chloride electrolyte using the Hoepfner method [5, 6]. Two installations with an output of up to 5 ton/day zinc were successfully operated: one from 1892–95 in Furfurt, Germany and the other from 1897–1924 in Winnington, England. Problems with obtaining suitable materials for anodes and diaphragms, and the emergence of the roast–sulphuric acid leach–electrowinning process for zinc recovery, led to the closing of these installations.

During the period 1955–59 the Russians conducted a detailed study on the problems involved in the electrolysis of zinc chloride to determine its prospects for industrial application [7–9]. In this work they determined the effects of current density, zinc and HCl concentrations and temperature on the current efficiency and deposit quality. The

0021–891X/79/050603–11 $03·10/0

effect of admixtures of Cu, Co, Ni and Sb as well as certain surface active additives on the current efficiency, cathode potential and deposit quality was also studied. Those results indicated that the deposit quality was dependent on the zinc and HCl concentration of the electrolyte as well as on the current density. From neutral solutions containing 10 g l^{-1} Zn fine-grained deposits were obtained only for current densities < 300 A m^{-2}; at higher current densities the deposits were dendritic and sponge-like. Slight acidification of the electrolyte (0·5 g l^{-1} HCl) yielded dense deposits for current densities to 1000 A m^{-2}. Increasing the acidity to 50 g l^{-1} HCl shifted dendrite formation to higher current densities, but the deposits were 'honeycombed'. Increasing the Zn concentration improved the deposit quality.

The influence of colloids and surface active substances on the electrolysis of $ZnCl_2$ was less effective than in the sulphate system [7]. According to Ralston [6], the use of glue as an addition agent in zinc chloride electrolyte, although it produces smoother plates, is not as successful in improving the condition of the cathodes as it is in the sulphate system.

The presence of admixtures of electropositive metals such as Cu, Co, Ni and Sb which lower the hydrogen overvoltage on Zn, in concentrations < 10 mg l^{-1} resulted in a sharp reduction in the current efficiency [7–9]. Impurities in the chloride electrolyte were arranged in the following order with respect to their harmful action:

$$Sb > Cu > Co > Ni.$$

The results of the Russian studies suggested the following conditions for electrowinning zinc from chloride electrolyte: $[Zn^{2+}] = 60$ g l^{-1}, [HCl] = 30 g l^{-1}, current density = 500 A m^{-2}, $T < 35°$ C, time < 24 h and impurity levels similar to those encountered in the corresponding sulphate system.

Although zinc electrolysis from sulphate electrolyte has received considerable attention industrially, it is only in the last few years that significant progress has been made in achieving more accurate control over the industrial electrowinning of zinc from sulphate electrolyte. It is now recognized, for example, that in addition to affecting current efficiency, impurities and additives in the electrolyte also have a major effect on the crystal growth of the zinc deposit and that there is a relationship between crystal growth and current efficiency. Recent studies on zinc electrolysis [10–15] have shown a definite correlation between zinc deposit morphology, the type and concentration of additives and/or impurities present in the electrolyte and the overpotential associated with zinc electrodeposition. As a result, it is possible to associate a given deposit morphology with a particular polarization (or overpotential) condition. The significance of these results is that a combination of zinc deposition polarization and deposit morphology (and orientation) observations, or possibly either individually, may be used to obtain valuable information on zinc electrolytes for application to industrial plant practice.

The objective of the present work was to determine the feasibility of electrowinning zinc from zinc chloride electrolyte. The initial phase of this study, the results of which are contained in this report, was to investigate the parameters (solution composition, impurities, temperature, current density, deposit morphology, etc.) affecting the recovery of high purity zinc from chloride electrolyte. An additional objective was to define a characteristic zinc deposit structure for chloride electrolyte and to determine the effect of additives and impurities on the deposit morphology and deposition polarization.

2. Experimental

2.1. *Electrolyte and additives*

The electrolyte was prepared from reagent grade zinc chloride ($ZnCl_2$). It had the following average analysis: Zn, 50 g l^{-1}; Cd, < 0·6 mg l^{-1}; Sb, < 0·5 mg l^{-1}; Co, < 0·1 mg l^{-1}; Ge, < 1 mg l^{-1}; As, < 1 mg l^{-1}; Ni, < 0·1 mg l^{-1}; Fe, < 0·05 mg l^{-1}; Pb, < 0·4 mg l^{-1}; Cu, 0·1 mg l^{-1}. For some tests the total chloride ion concentration was increased to 4 M by adding NaCl. The additives studied included HCl, animal glue, gum arabic, Jaguar C-13*, tetraethylammonium chloride (TEACl) and tetrabutylammonium chloride (TBACl). They were added to the electrolyte as aliquots from their respective

* Jaguar is Stein-Hall's registered trademark applied to Guar gum and Guar derivatives. Guar gum, a galactomanan, is a high molecular weight carbohydrate polymer or polysaccharide made up of many mannone and galoctone units. Jaguar C-13 is a Guar gum derivative.

aqueous stock solutions. The metallic impurities Cu, Co, Cd, Ni, Fe(II) and Fe(III) were added to the electrolyte as aliquots from stock solutions prepared from their respective chloride salts. Antimony additions were made as potassium antimony tartrate solution and lead was added as a lead acetate solution.

2.2. *Electrolysis cells*

Both conventional and diaphragm cells were used in this study. The conventional cell was the same as that employed in previous studies using zinc sulphate electrolyte [13–15]. The diaphragm cell was fabricated from 0·64 cm thick polycarbonate. It consisted of a central cathode compartment separated from the anode compartments by diaphragms fabricated from Nafion (Dupont). The anodes were either graphite rods or Pt sheet and the cathode was fabricated from commercial purity Al sheet and was mounted in the cells so that the total deposit area was 12·9 cm^2.

2.3. *Electrolysis conditions*

Operating conditions of 538 A m^{-2} (50 ASF) and 35° C were used for most of the experiments although additional tests were conducted at 269 A m^{-2} (25 ASF) and 807 A m^{-2} (75 ASF) and at 40° C, 50° C and 60° C. All tests were run for one hour total electrolysis time. The electrolyte was agitated with a glass stirrer at a constant speed of 2100 rev min^{-1}.

2.4. *Deposit examination*

Sections of the deposits were examined by X-ray diffraction (XRD) to determine their preferred orientation relative to the ASTM standard for zinc powder and by scanning electron microscopy (SEM) to determine their surface morphology. Deposit cross-sections were examined by optical microscopy (OM) techniques.

2.5. *Polarization studies*

Current–potential curves for zinc deposition were obtained using a Wenking potentiostat model 70HP10 driven at a rate of 1 mV s^{-1} by a Wenking model VSG72 voltage scan generator. The effect of glue, gum arabic, Jaguar C-13, TEACl and TBACl on the zinc deposition i–V curve was determined over the potential range − 800 to − 2300 mV versus a saturated calomel reference electrode (SCE). The i–V curves, obtained for the cathodic direction only, were stationary and reproducible under the experimental conditions.

3. Results and discussion

3.1. *Addition-free zinc chloride electrolyte*

The SEM photomicrograph, Fig. 1a, shows the typical morphology of zinc deposits obtained under a variety of experimental conditions using addition-free zinc chloride electrolyte; these experimental conditions are summarized in Table 1. The zinc deposit consists of clusters of large, poorly defined hexagonal platelets with large voids occurring at the boundaries of the platelet clusters. The deposit cross-section shown in Fig. 1b reveals that these voids penetrate to the aluminium substrate. The crystallographic orientation for the zinc deposits obtained under all the conditions in Table 1 was highly preferred (0 0 2) (1 0 3) (1 0 5). This is typical of basal orientation in which the zinc platelets are aligned parallel to the aluminium substrate.

The average current efficiency for the 1 h zinc

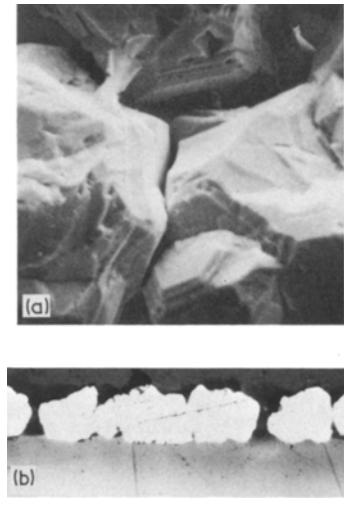

Fig. 1. (a) SEM photomicrograph showing the morphology (× 840) and (b) OM photomicrograph showing the cross-section of a 1 h zinc deposit obtained from addition-free zinc chloride electrolyte at 538 A m^{-2} (× 48).

Table 1. Experimental conditions for addition-free electrolytes

Current density ($A\,m^{-2}$)	*Zn^{2+}, as $ZnCl_2$* ($g\,l^{-1}$)	*Temperature* (° C)	*Anodes*
269,538,807	50	35, 50, 60	Pt, graphite
269,538,807	50	35	graphite*
269,538,807	100	35	graphite
269,538,807	50†	35	graphite
269,538,807‡	50	35	graphite

* bagged anodes, standard cell
† total $[Cl^-] = 4$ M with addition of NaCl
‡ diaphragm cell

deposits obtained under the conditions listed in Table 1 was 80%; it did not change significantly when a diaphragm cell was employed. The average cell voltage was 4·4 V for an applied current density of 538 $A\,m^{-2}$; it also did not vary with the type of cell used.

3.2. *Effect of hydrogen ion concentration*

The addition of HCl to the zinc chloride electrolyte resulted in a substantially improved zinc deposit. The HCl was varied between 0 and 2·4 M. The optimum hydrogen ion concentration in terms of deposit morphology and current efficiency was found to be 0·24 M. The zinc deposit morphology obtained at 538 $A\,m^{-2}$ from a zinc chloride electrolyte containing 0·24 M H^+ for deposition times of 30 min and 60 min is shown in Figs. 2a and c, respectively. The zinc platelets are better defined and there are no voids in the deposit (Figs. 2b and d) as compared to that obtained from the addition-free electrolyte (Fig. 1a).

The presence of 0·24 M H^+ increased the current efficiency to about 90% and lowered the cell voltage to 4·0 V in both the conventional and diaphragm cells. Variations in $[H^+]$ for current densities of 269, 538 and 807 $A\,m^{-2}$ did not alter the preferred deposit orientation which remained (0 0 2) (1 0 3) (1 0 5); however, increasing $[H^+]$ preferentially increased the (0 0 2) orientation whereas the (1 0 3) and (1 0 5) orientations remained essentially constant at each value of the current density.

For comparative purposes, the characteristic zinc deposit morphology obtained from acid zinc sulphate electrolyte over a wide range of experimental conditions [11] is shown in Fig. 2e. It can be seen that the deposit is characterized by smaller size, hexagonal zinc platelets which are oriented at intermediate angles to the aluminium substrate The preferred orientation for this deposit morphology is (1 1 2) (1 1 4) (1 0 2). Sato [16] reported a (1 1 4) orientation for a zinc deposit obtained from acid sulphate electrolyte.

It is interesting to note that the addition of

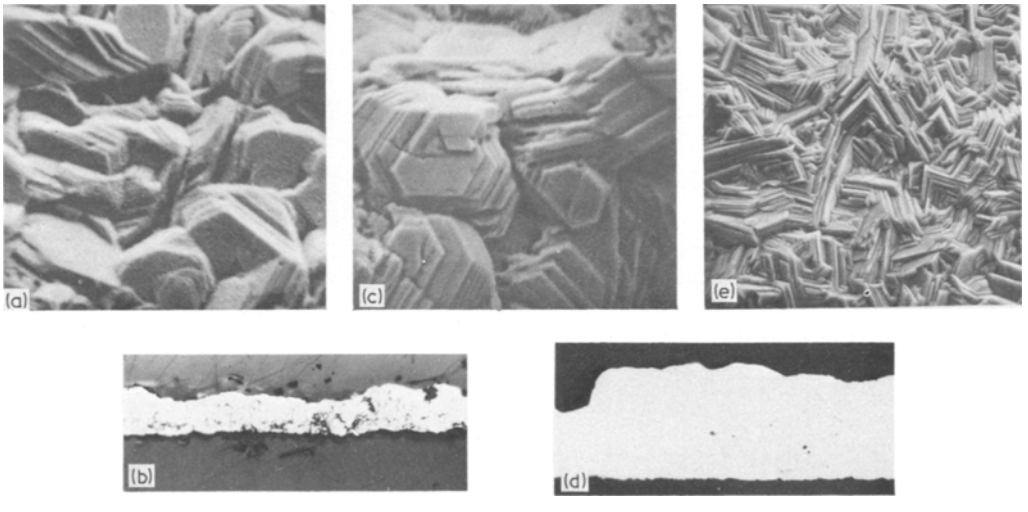

Fig. 2. (a) and (c) SEM photomicrographs (at 30 min and 1 h, respectively) showing the morphology (× 840) and (b) and (d) OM photomicrographs (at 30 min and 1 h, respectively) showing the cross-section of zinc deposits obtained from zinc chloride electrolyte containing 0·24 M H^+ at 538 $A\,m^{-2}$ (× 48); (e) SEM photomicrograph showing the morphology of a zinc deposit obtained from an addition-free acid zinc sulphate electrolyte after 1 h (× 840).

chloride ion to acid zinc sulphate electrolyte changes the zinc deposit orientation to a basal type in which the zinc platelets are aligned parallel to the aluminium cathode. Fukubayashi *et al.* [17] observed that the addition of HCl (100–2000 $mg\,l^{-1}$) to acid zinc sulphate electrolyte resulted in a zinc deposit having an (0 0 2) preferred orientation. In the present work, increasing $[H^+]$ by HCl additions increased the (0 0 2) orientation in preference to (1 0 3) and (1 0 5). MacKinnon *et al.* [18] also studied the effect of chloride ion on the morphology and orientation of zinc deposits obtained from acid sulphate electrolyte. The addition of chloride ion to 500 $mg\,l^{-1}$ as NaCl changed the deposit orientation from (1 1 2) (1 1 4) (1 0 2) to (1 0 3) (1 0 5).

3.3. *Effect of glue additions*

The addition of glue to zinc chloride electrolyte containing various $[H^+]$ had a significant effect on the zinc deposit morphology. Typical glue addition morphologies are shown in the SEM photomicrographs in Figs. 3a and c. As indicated by Fig. 3a, the addition of 80 $mg\,l^{-1}$ glue to a zinc chloride electrolyte containing 0·24 M H^+ caused the zinc platelets to become vertically aligned to the aluminum substrate, which corresponded to a (1 1 0) preferred deposit orientation as determined by XRD analysis.

Increasing the $[H^+]$ to 0·48 M in the presence of 60 $mg\,l^{-1}$ glue resulted in another type of deposit morphology (Fig. 3c) which bears some resemblance to that obtained under optimum conditions from sulphate electrolyte (Fig. 2e). In this case, the zinc platelet size is substantially reduced and the deposit has a random or intermediate orientation, i.e. (1 0 1) (1 0 2) (1 0 3). Further, the respective cross-sections shown in Figs. 3b and d, indicate that this morphology type (Fig. 3c) results in an even deposit growth as compared to that of Fig. 3a.

In addition to improving the deposit morphology, the presence of glue in the acidified zinc chloride electrolyte increased the current efficiency to better than 90%. The cell voltage remained at 4·0 V for an applied current density of 538 $A\,m^{-2}$. These results were obtained using both a diaphragm and a conventional electrolysis cell.

3.4. *Effect of addition agents other than glue*

The effect of addition agents other than glue on the zinc deposit morphology and orientation was also studied. These additives, which included gum arabic, Jaguar C-13, tetraethylammonium chloride (TEACl) and tetrabutylammonium chloride (TBACl), were evaluated over the concentration range 0–60 $mg\,l^{-1}$.

The addition of gum arabic had a significant effect on the zinc deposit morphology (Fig. 4a). The deposit grain size was substantially reduced,

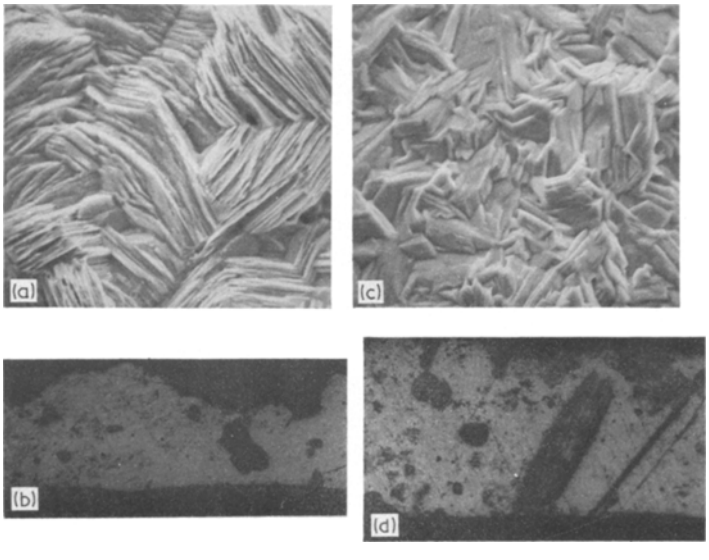

Fig. 3. (a) and (c) SEM photomicrographs showing the morphology (× 840) and (b) and (d) OM photomicrographs showing the cross-section (× 48) of 1 h zinc deposits obtained from zinc chloride electrolyte containing H^+ and glue at 538 $A\,m^{-2}$: (a) and (b) 0·24 M H^+, 80 $mg\,l^{-1}$ glue; (c) and (d) 0·48 M H^+, 60 $mg\,l^{-1}$ glue.

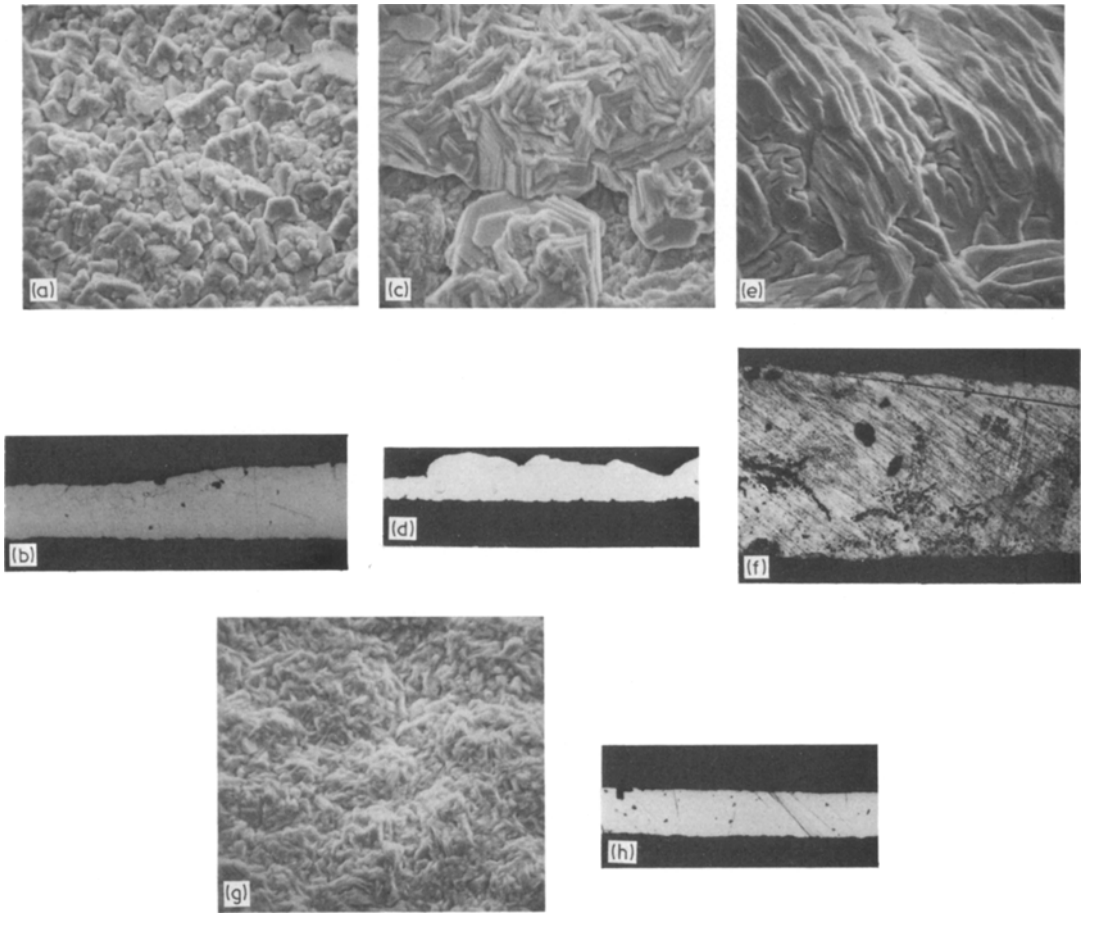

Fig. 4. (a), (c), (e) and (g) SEM photomicrographs showing the morphology (× 840) and (b), (d), (f) and (h) OM photomicrographs showing the cross-section (× 48) of 1 h zinc deposits obtained from zinc chloride electrolyte containing 0·24 M H^+ and various organic additives at 538 A m^{-2}. (a) and (b) 45 mg l^{-1} gum arabic; (c) and (d) 30 mg l^{-1} TEACl; (e) and (f) 30 mg l^{-1} Jaguar C-13; (g) and (h) 45 mg l^{-1} TBACl.

although the orientation remained (0 0 2) (1 0 3) preferred (Table 2). The deposit cross-section was smooth and compact (Fig. 4b). TEACl addition was less effective in reducing the deposit grain size (Fig. 4c), and the deposit orientation remained strongly preferred (0 0 2). The deposit cross-section (Fig. 4d), indicates uneven growth. Increasing amounts of Jaguar C-13 in the electrolyte produced the morphology type shown in Fig. 4e which shows the deposit to consist of poorly defined platelets aligned at intermediate angles to the aluminium substrate. The lack of grain refinement is further indicated by the thickness of the cross-section shown in Fig. 4f.

TBACl had a strong influence on the zinc deposit morphology (Fig. 4g). In this case, the morphology was similar to that obtained for the glue-addition electrolyte (cf. Fig. 3a), in which the zinc platelets were aligned perpendicular to the aluminium substrate, but the grain size is more refined. This is corroborated by the smooth, compact cross-section shown in Fig. 4h.

The crystallographic orientations for deposits obtained from electrolytes containing these additives are summarized in Table 2. The results are in good agreement with the respective morphology types; gum arabic and TEACl additions did not affect the deposit orientation which remained (0 0 2), Jaguar C-13 additions resulted in an intermediate or (1 1 2) (1 1 4) orientation while TBACl additions produced deposits having a vertical or (1 1 0) orientation. Gum arabic, which did not

Table 2. Effect of various addition agents on the orientation of zinc deposits obtained at 538 A m^{-2}. (Electrolysis conditions: 50 g l^{-1} Zn, 0·24 M H^+, 40° C)

Additive concentration (mg l^{-1})				*Orientation**	*Corresponding figure in text*
Gum arabic	*Jaguar C-13*	*TEACl*	*TBACl*		
30	–	–	–	(1 0 3) (0 0 2)	–
45	–	–	–	(0 0 2) (1 0 3)	4a, 4b
60	–	–	–	–	–
–	30	–	–	(1 0 3) (1 0 5)	4e, 4f
–	45	–	–	(1 1 2) (1 1 4)	–
–	60	–	–	(1 0 3) (1 1 4)	–
–	–	30	–	–	4c, 4d
–	–	45	–	(0 0 2)	–
–	–	60	–	(0 0 2)	–
–	–	–	30	(1 1 0)	–
–	–	–	45	(1 1 0)	4g, 4h
–	–	–	60	(1 1 0)	–

* Relative to ASTM standard for zinc powder

alter the deposit orientation, also tended to give a lower current efficiency (87%) than glue (92%); the presence of TBACl, which caused increased grain refinement, gave a higher current efficiency (94%) than glue.

3.5. *Polarization studies*

The cathodic polarization curve for zinc deposition onto aluminium from chloride electrolyte containing 0·24 M H^+ (as HCl) was obtained at 40° C. This polarization curve was the basis of comparison for polarization curves obtained from electrolytes containing glue, Jaguar C-13, gum arabic, TEACl and TBACl in addition to 0·24 M H^+ under similar experimental conditions. The degree of polarization caused by these various addition agents was obtained by comparing the current, i, to that obtained for the addition-free, acidified electrolyte at a given value of the cathodic potential. The data are summarized in Table 3 for four values of the cathodic potential.

A comparison of the data in Table 3 indicates that TBACl causes the strongest polarization since it gives the smallest currents at the various selected cathode potentials. Gum arabic and glue have similar polarization characteristics. Jaguar C-13 has only a slight polarizing effect on the reaction. In terms of increasing polarization, the various addition agents may be arranged in the order:

$$\text{TBACl} > \text{glue} \approx \text{gum arabic} > \text{TEACl} > \text{Jaguar C-13}.$$

The strong polarizing effect of TBACl corresponds to a vertical or perpendicular (1 1 0) deposit orientation. Glue, which has somewhat weaker polarization properties, gives intermediate to vertical orientation, (1 0 1) (1 1 0). The weak polarizing effect of Jaguar C-13 results in a basal to intermediate orientation, (0 0 2) (1 1 4) (1 1 2). Thus the trend in deposit orientation in relation to the polarization is as follows:

basal

(0 0 2) ← (1 0 5)

←

decreasing polarization

intermediate *perpendicular*

(1 0 3) ↔ (1 0 2) (1 1 4) (1 1 2) ↔ (1 0 1) → (1 1 0)

⟶

increasing polarization

Although both gum arabic and TEACl gave stronger polarization than Jaguar C-13 (Table 3), they did not change the deposit orientation (Table 2) and therefore do not fit into the above trend. Gum arabic did, however, significantly reduce the deposit grain size. TEACl additions did not change the physical appearance of the deposit which, like the addition-free deposit, was coarsely crystalline. TBACl and glue gave smooth fine-grained deposits.

Table 3. Zinc deposition polarization current as a function of various addition agents (Electrolysis conditions: 50 g l^{-1} Zn, 0·24 M H^+, 40° C)

Addition agent	*E* (mV versus SCE) *at current*			
	— 1100 (mA)	*— 1500* (mA)	*— 1900* (mA)	*— 2300* (mA)
none	125	863	1600	2480
60 mg l^{-1} glue	80	775	1460	2235
60 mg l^{-1} Jaguar C-13	100	850	1600	2400
60 mg l^{-1} gum arabic	100	775	1500	2250
60 mg l^{-1} TEACl	100	813	1525	2405
60 mg l^{-1} TBACl	75	650	1200	2000

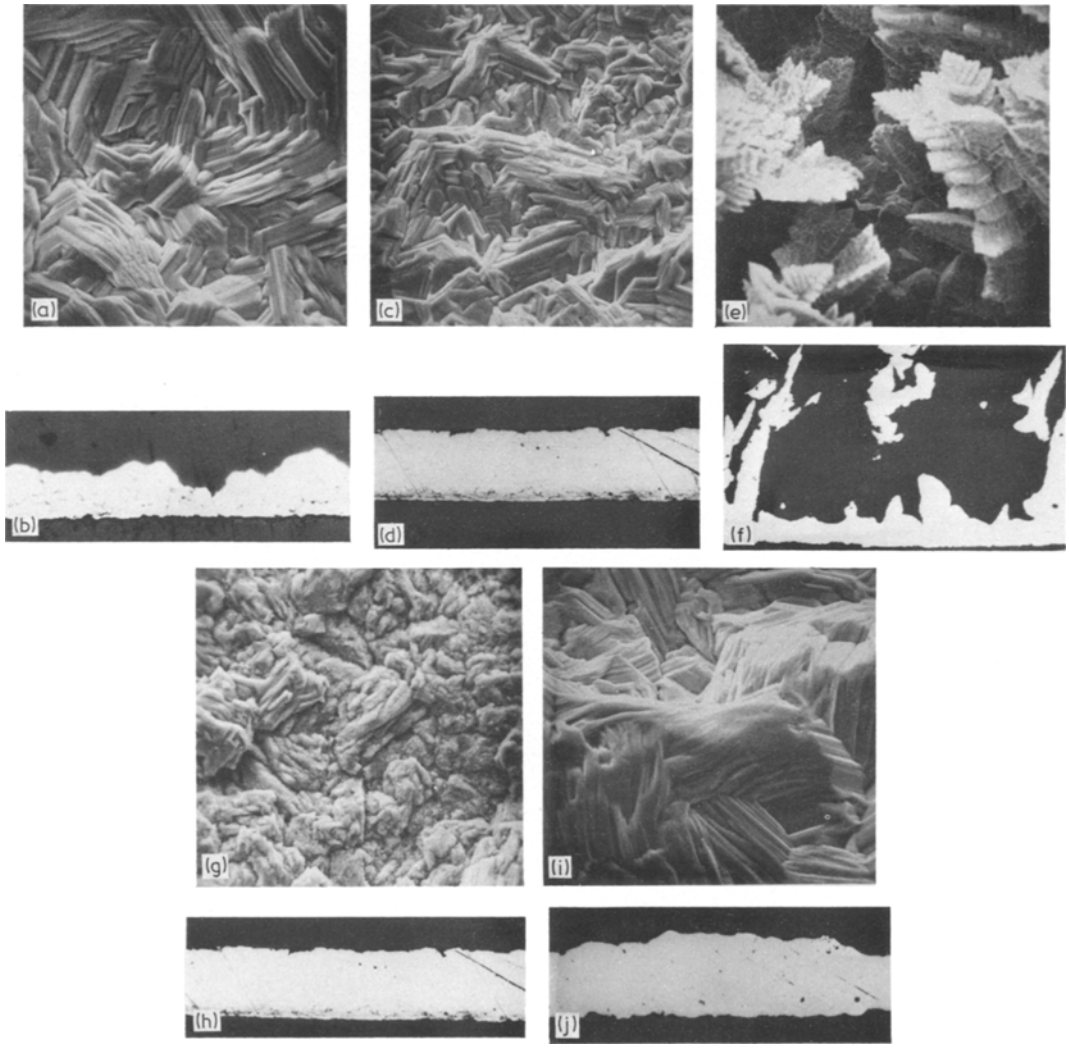

Fig. 5. (a), (c), (e), (g) and (i) SEM photomicrographs showing the morphology [× 840 except (e) × 210] (b), (d), (f), (h) and (j) OM photomicrographs showing the cross-section (× 48) of 1 h zinc deposits obtained from zinc chloride electrolyte containing 0·24 M H^+, 60 mg l^{-1} glue and various metallic impurities at 538 A m^{-2}: (a) and (b) 10 mg l^{-1} Co; (c) and (d) 2 mg l^{-1} Cu; (e) and (f) 50 mg l^{-1} Cu; (g) and (h) 50 mg l^{-1} Pb; (i) and (j) 0·10 mg l^{-1} Sb.

3.6. *Effect of metallic impurities*

The effect of the indivdual metallic impurities Cu, Co, Cd, Ni, Fe(II), Fe(III), Pb and Sb, on the morphology of zinc deposits obtained at 538 A m^{-2} from zinc chloride electrolyte containing 60 mg l^{-1} glue and 0·24 M H^+ was also studied. The addition of Cd, Co, Ni, Fe(II) and Fe(III) to the electrolyte had similar effects on the deposit morphology, a typical example of which is shown in Fig. 5a. This morphology type which is characterized by a (1 1 0) (1 1 2) orientation, persisted over a wide range of impurity concentrations. The deposit cross-section shown in Fig. 5b indicates an

Table 4. Effect of impurity concentration on the zinc deposit orientation and deposition current efficiency. (Electrolysis conditions: 50 g l^{-1} Zn, 0·24 M H^+, 60 mg l^{-1} glue, 40° C, 538 A m^{-2})

Impurity	*Impurity concentration* (mg l^{-1})	*Orientation**	*Current efficiency* (%)
Cu	2	(1 1 2) (1 0 2)	91·4
	5	(1 0 2)	89·5
	10	(1 1 2)	86·6
	50	(0 0 2)	85·9
Co	2	(1 1 0) (1 1 2)	88·1
	5	(1 1 0) (1 1 2)	89·7
	10	(1 1 0) (1 1 2)	84·6
	50	(1 1 0)	85·7
	100	(1 1 0) (1 1 2)	82·0
Cd	2	(1 1 2) (1 1 0)	81·3
	5	(1 1 2) (1 1 0)	73·9
	10	(1 1 2) (1 1 0)	86·4
	50	(1 1 2) (1 1 4)	86·2
Fe(II)	2	(1 1 2)	86·5
	5	(1 1 0)	85·6
	10	(1 1 0)	83·8
	50	(1 1 0)	87·0
	100	(1 1 2)	78·7
	300	(0 0 2)	48·4
Fe(III)	2	(1 1 0) (1 1 2)	88·2
	5	(1 1 0) (1 1 2)	86·4
	10	(1 1 0) (1 1 2)	87·7
	50	(1 1 0) (1 1 2)	86·6
	100	(1 0 3) (1 0 2)	88·1
	200	(1 1 2)	59·9
	300	(1 0 2)	73·9
Ni	2	(1 1 0) (1 1 2)	85·4
	5	(1 1 0) (1 1 2)	85·1
	10	(1 1 0) (1 1 2)	86·8
	50	(1 1 2)	83·1
	100	(1 0 3) (1 0 2)	79·7
Pb	2	(1 0 1)	87·5
	5	(1 0 1)	82·5
	10	(1 0 1)	85·9
	50	(1 0 1)	84·1
Sb	0·08	(1 1 0)	85·0
	0·10	(1 1 2) (1 1 0)	82·8
	0·20	(1 1 0)	64·1
	0·50	–	11·1

* Relative to ASTM standard for Zn powder

uneven growth. The effects of impurity concentration on the deposit orientation and the corresponding current efficiency are summarized in Table 4. For concentrations of Co and Fe(II) up to 100 mg l^{-1} and Cd, Fe(III) and Ni to 50 mg l^{-1}, the deposit orientation was intermediate to vertical, i.e., (1 1 2) (1 1 0) and the current efficiency averaged > 80%. For higher concentrations of these metallic impurities, the orientation tended to be intermediate to basal, e.g., (1 0 3) (1 0 2) for 100 mg l^{-1} Fe(III) and (0 0 2) for 300 mg l^{-1} Fe(II) (Table 4). The current efficiency generally decreased at these higher impurity concentrations.

The effect of Cu was somewhat different in that for the concentration range 2–10 mg l^{-1}, the morphology type (Fig. 5c) was characterized by an intermediate orientation, (1 1 2) (1 0 2), which resulted in an even deposit growth as indicated by the deposit cross-section (Fig. 5d). The addition of 50 mg l^{-1} Cu resulted in a basal (0 0 2) oriented deposit which exhibited a high degree of dendritic growth (Fig. 5c). This dendritic growth is equally apparent in the deposit cross-section (Fig. 5f).

The addition of Pb to the electrolyte resulted in zinc deposits which had a 'lead-type' morphology [14] as shown in Fig. 5g. Even for Pb levels as low as 2 ppm, the deposit morphology indicated a lead content in the deposit of ~ 0·02% [14]. The preferred orientation was (1 0 1) for all Pb concentrations studied and the CE averaged about 85%. The corresponding cross-section (Fig. 5h) shows a smooth, even deposit. It has been reported [19] that lead acetate addition to either alkaline or acid zinc electrolyte inhibits the irregular growth of zinc deposits.

The addition of Sb resulted in strongly preferred (1 1 0) oriented deposits at lower concentrations (Table 4). A typical morphology is shown in the SEM photomicrograph of Fig. 5i, which reveals poorly defined Zn platelets vertically oriented to the aluminium substrate. The cross-section, (Fig. 5j) reveals uneven growth. Increasing antimony concentrations beyond 0·10 mg l^{-1} results in severe re-solution of the zinc deposit and this is reflected by the low CE values (Table 4).

4. Conclusions

A zinc deposit structure obtained from both addition-free and acid aqueous zinc chloride electrolytes, having a characteristic morphology and orientation (0 0 2) (1 0 3) (1 0 5), was identified. This deposit was entirely unlike that obtained from the corresponding addition-free acid zinc sulphate electrolyte.

Macroscopically, the zinc deposit from addition-free zinc chloride electrolyte was sponge-like and contained voids which extended to the aluminium cathode. The addition of HCl, 0·24–0·48 M H^+ (9–17 g l^{-1} HCl), eliminated these voids but did not substantially affect the deposit surface morphology or orientation.

The addition of glue and other organic levelling agents had a strong effect on the deposit morphology and orientation as well as on zinc deposition polarization. Although various combinations of H^+ and animal glue had beneficial effects on the deposits, tetrabutylammonium chloride appeared to be a superior additive. The results of the polarization studies indicated only a limited correlation between deposit orientation and the degree of polarization caused by the various addition agents present in the zinc chloride electrolyte.

In general, the results obtained from the study of the effects of individual metallic impurities on 1 h zinc deposits obtained from zinc chloride electrolyte containing optimum H^+ and glue concentrations indicate that rather high levels of these impurities can be tolerated, as is the case for the sulphate electrolyte containing similar glue levels. The low tolerance to antimony (0·1 mg l^{-1}) is also similar to that observed in the sulphate system.

Acknowledgements

The authors wish to express their thanks to Dr R. C. Kerby, Cominco Ltd, who provided many helpful comments and suggestions to this work. Thanks are also due to Cominco Ltd for supplying the glue and cathode aluminium and to Dr R. Packwood, CANMET, for providing the SEM facilities. J. M. Stewart and E. J. Murray, CANMET, did the X-ray diffraction measurements and Y. Bourgoin, CANMET, prepared the polished sections for optical microscopy. One of us (V.I.L.) gratefully acknowledges the National Research Council, Canada for awarding a fellowship.

References

[1] H. W. Parsons and G. M. Ritcey, *Northern Miner* **63 (37)** (1977) D-20.
[2] J. M. R. Vega and E. D. Nogueira, US Patent 3923 976 (2 December, 1975).
[3] T. H. Tunley, P. Köhler and T. D. Sampson, National Institute for Metallurgy, Report No. 1685 (1976) p. 12.
[4] A. K. Haines, T. H. Tunley, W. A. M. Te Riele, F. L. D. Cloete and T. D. Sampson, *J. South African Inst. Min. Met.* (1973) 149.
[5] E. Günther, 'Die Darstellung des Zinks auf Elektrolytischen Wege' Wilhelm Knopp, Halle (1904).
[6] O. C. Ralston, 'Electrolytic Deposition and Hydrometallury of Zinc', McGraw-Hill Book Co., Inc., New York (1921) Ch. 7.
[7] E. A. Kalinovskii and V. V. Stender, *Ukr. Khim. Zh.* **23** (1957) 384.
[8] A. F. Nikivorov and V. V. Stender, *Vestn. Akad. Nauk Kaz, S.S.R.* **10** (1958) 42.
[9] A. F. Nikivorov and V. V. Stender, *Ukr. Khim. Zh.* **25** (1959) 18.
[10] D. J. Robinson and T. J. O'Keefe, *J. Appl. Electrochem.* **6** (1976) 1.
[11] B. A. Lamping and T. J. O'Keefe, *Metall. Trans.* **7B** (1976) 551.
[12] R. C. Kerby, H. E. Jackson, T. J. O'Keefe and Yar-Ming Wang, *ibid* **8B** (1977) 661.
[13] D. J. MacKinnon and J. M. Brannen, *J. Appl. Electrochem.* 7 (1977) 451.
[14] D. J. MacKinnon, J. M. Brannen and R. C. Kerby, *J. Appl. Electrochem.* 9 (1979) 55.
[15] *Idem, ibid* 9 (1979) 71.
[16] R. Sato, *J. Electrochem. Soc.* **106** (1959) 206.
[17] H. Fukubayashi, T. J. O'Keefe and W. C. Clinton, USBM Report of Investigations, RI 7966 (1974) 26.
[18] D. J. MacKinnon, J. M. Brannen and V. I. Lakskmanan, to be published.
[19] J. Bressan and R. Wiart, *J. Appl. Electrochem.* 7 (1977) 505.